The American Journal of Pathology, Vol. 194, No. 7, July 2024

ELSEVIER

The American Journal of
PATHOLOGY
ajp.amjpathol.org

OCULAR PATHOBIOLOGY

Enhanced Optic Nerve Expansion and Altered Ultrastructure of Elastic Fibers Induced by Lysyl Oxidase Inhibition in a Mouse Model of Marfan Syndrome

Hang-Jing Wu,* Evan Krystofiak,† John Kuchtey,* and Rachel W. Kuchtey*‡

From the Vanderbilt Eye Institute, Vanderbilt University Medical Center, Nashville; and the Cell Imaging Shared Resource† and the Department of Molecular Physiology and Biophysics,‡ Vanderbilt University, Nashville, Tennessee*

Accepted for publication March 11, 2024.

Address correspondence to Rachel W. Kuchtey, M.D., Ph.D., Vanderbilt Eye Institute, Vanderbilt University Medical Center, 2311 Pierce Ave., Nashville, TN 37232-8808. E-mail: rachel.w.kuchtey@vumc.org.

Two major constituents of exfoliation material, fibrillin-1 and lysyl oxidase-like 1 (encoded by *FBN1* and *LOXL1*), are implicated in exfoliation glaucoma, yet their individual contributions to ocular phenotype are minor. To test the hypothesis that a combination of *FBN1* mutation and *LOXL1* deficiency exacerbates ocular phenotypes, the pan—lysyl oxidase inhibitor β-aminopropionitrile (BAPN) was used to treat adult wild-type (WT) mice and mice heterozygous for a missense mutation in *Fbn1* ($Fbn1^{C1041G/+}$) for 8 weeks and their eyes were examined. Although intraocular pressure did not change and exfoliation material was not detected in the eyes, BAPN treatment worsened optic nerve and axon expansion in $Fbn1^{C1041G/+}$ mice, an early sign of axonal damage in rodent models of glaucoma. Disruption of elastic fibers was detected only in $Fbn1^{C1041G/+}$ mice, which increased with BAPN treatment, as shown by histologic and immunohistochemical staining of the optic nerve pia mater. Transmission electron microscopy showed that $Fbn1^{C1041G/+}$ mice had fewer microfibrils, smaller elastin cores, and a lower density of elastic fibers compared with WT mice in control groups. BAPN treatment led to elastin core expansion in both WT and $Fbn1^{C1041G/+}$ mice, but an increase in the density of elastic fiber was confined to $Fbn1^{C1041G/+}$ mice. LOX inhibition had a stronger effect on optic nerve and elastic fiber parameters in the context of *Fbn1* mutation, indicating the Marfan mouse model with LOX inhibition warrants further investigation for exfoliation glaucoma pathogenesis. *(Am J Pathol 2024, 194: 1317—1328; https://doi.org/10.1016/j.ajpath.2024.03.002)*

Exfoliation syndrome (XFS) is an age-related systemic disease characterized by the accumulation of extracellular fibrillar aggregates throughout the body.[1,2] Clinically, XFS is associated with cardiac vascular disease and others, but the most prominent manifestations occur in the eye.[3] The fibrillar aggregates, termed exfoliation material (XFM), have a characteristic distribution and appearance on the surface of the anterior lens capsule and pupillary margin, which can be detected readily by slit lamp examination. Accumulation of XFM in the aqueous humor outflow pathway leads to increased intraocular pressure (IOP), and, eventually, exfoliation glaucoma (XFG).[4] XFG also can develop in patients with XFS without obvious increased IOP, which likely is owing to abnormal elastic fibers in the optic nerve head, particularly the lamina cribrosa of the optic nerve,[5] the initial site for glaucomatous optic nerve damage.[6—8]

Genome-wide association studies have identified *LOXL1* among seven genomic loci associated with XFS.[9,10] *LOXL1* encodes lysyl oxidase-like 1 protein (LOXL1), which is a member of the LOX family of secreted enzymes, including LOX and LOXL1 to 4.[11] LOX family members are highly related in structure, consisting of conserved C-terminal catalytic domains that oxidize primary amine substrates to form reactive aldehydes and variable N-terminal domains, which are important for substrate recognition and enzyme

Supported by National Eye Institute grant R01EY020894 (R.W.K.), The Glaucoma Foundation (R.W.K.), Vanderbilt Vision Research Center grant P30EY008126, and a Departmental Unrestricted Award from Research to Prevent Blindness, Inc. Imaging was supported through the Vanderbilt University Medical Center Cell Imaging Shared Resource core facility. Electron microscopy was performed using the Vanderbilt Cell Imaging Shared Resource, which is supported by NIH grants CA68485, DK20593, DK58404, and DK59637.

https://doi.org/10.1016/j.ajpath.2024.03.002

maturation. LOXL, particularly LOXL1, cross-links monomers of soluble tropoelastin into insoluble elastin, promoting the formation and maintenance of extracellular elastic fibers.[12] Elastic fibers are composed of an amorphous elastin core surrounded by a sheath of microfibrils, which are composed primarily of fibrillin-1 (encoded by *FBN1*). Elastic fibers serve vital functions and are nearly ubiquitous in vertebrates, endowing connective tissues such as lungs, arteries, and skin, with the critical properties of elasticity and resilience. Stable formation and proper function of elastic fiber requires microfibrils, which serve as scaffolding for elastin deposition and core formation.[13] Abnormal microfibrils caused by *FBN1* mutations results in characteristic elastic fiber fragmentation in the aortic wall of Marfan syndrome patients.[14] In addition to cross-linking elastin, a role for LOXL1 in cross-linking collagen has been suggested as well.[15] More recently, ultrastructural alteration of elastic fibers and collagen fibrils in the peripapillary sclera of $Loxl1^{-/-}$ mice was demonstrated.[16]

Among the variety of XFM components detected in the eyes of patients with XFS, fibrillin-1 and LOXL1 are reported consistently by independent studies using different techniques,[2,17–21] further implying their roles in XFG pathogenesis. Mice heterozygous for the Tight skin (*Tsk*) mutation of *Fbn1* ($Fbn1^{Tsk/+}$) develop glaucoma-related phenotypes at an advanced age, such as reduced retinal ganglion cell (RGC) function, or expanded optic nerve and RGC axons, accompanied by thinning of optic nerve pia mater in the setting of normal IOP.[22,23] The expanded optic nerve and axons observed in $Fbn1^{Tsk/+}$ mice are consistent with the report that optic nerve enlargement precedes axonal loss in an experimental rodent model and the DBA2/J mouse model of glaucoma.[24,25]

Optic nerve enlargement phenotypes for $Loxl1^{-/-}$ mice also have been reported,[16] and the same phenotype in mice heterozygous for a missense mutation in *Fbn1* ($Fbn1^{C1041G/+}$) was observed. $Fbn1^{C1041G/+}$ mice have been used widely as a model for human patients with mild Marfan syndrome (MFS).[26] The hallmark of MFS is aorta dilation and dissection with characteristic findings of fragmented elastic fibers in the aorta wall. $Fbn1^{C1041G/+}$ mice recapitulate the cardiac phenotypes faithfully, although at much advanced age, hence commonly referred to as a mild MFS mouse model. A study conducted by Busnadiego et al[27] demonstrated that inhibition of lysyl oxidase activity with β-aminopropionitrile (BAPN) in $Fbn1^{C1041G/+}$ mice hastened the development of aorta dilation. LOX and LOXL1 expression are up-regulated in the aorta of patients with MFS and $Fbn1^{C1041G/+}$ mice, indicating close interaction of fibrillin-1 and LOX/LOXL1.[27] In addition to characteristic cardiac findings, patients with MFS have a high prevalence of ectopia lentis caused by zonular instability,[14] a shared ocular phenotype of XFS.[28] This sharing of zonule phenotype between MFS and XFS further supports functional overlap between fibrillin-1 and LOXL1. Interestingly, although lens zonules are composed predominately of elastin-free fibrillin microfibril bundles, a recent proteomic study found that in addition to fibrillin-1 being the most abundant, LOXL1 also is expressed highly in the zonules.[29]

Fibrillin-1 and LOXL1 are two major components of XFM,[2,17–21] yet the causality of defects in each component individually has not been established for XFG. A lack of LOXL1 in mice results in some ocular phenotypes of XFS, but neither optic nerve degeneration nor XFM have been detected.[16] Here, it was hypothesized that fibrillin-1 deficiency combined with pharmacologic inactivation of LOX activity would result in more severe ocular phenotypes, similar to that observed in the cardiovascular system.[27] To that end, wild-type (WT) and $Fbn1^{C1041G/+}$ mice were treated with BAPN. Worsening optic nerve enlargement and worsening of RGC axon expansion accompanied with a structural change of elastic fibers in the optic nerve pia mater of BAPN-treated $Fbn1^{C1041G/+}$ mice were detected.

Materials and Methods

Mice

All animal studies were performed in accordance with the Association for Research in Vision and Ophthalmology guidelines for the Use of Animals in Ophthalmic and Vision Research and were approved by the Institutional Animal Care and Use Committee of Vanderbilt University Medical Center. Male mice heterozygous for the C1041G mutation of *Fbn1* and female mice homozygous for wild-type *Fbn1* on a C57BL/6J background were bred to produce cohorts of experimental animals heterozygous for the C1041G mutation of *Fbn1*, hereafter referred to $Fbn1^{C1041G/+}$, and control animals homozygous for wild-type *Fbn1* (hereafter referred to as WT). The genotype of each experimental mouse was determined at weaning. Animals were housed in a facility operated by the Vanderbilt University Division of Animal Care, with a 12/12-hour light/dark cycle and *ad libitum* access to food and water.

BAPN Treatment

Wild-type and $Fbn1^{C1041G/+}$ mice at 9 months of age were injected intraperitoneally with either BAPN (catalog #A3134; Sigma-Aldrich, St. Louis, MO), which inhibits cross-linking activity of all LOX family members (Lox and Loxl1 to 4) *in vivo*,[30] or phosphate-buffered saline (PBS) as vehicle control. BAPN was dissolved in PBS and injected at a dose of 300 mg/kg.[27] Injections were performed daily for 8 weeks.

IOP Measurement

Mice were anesthetized by isoflurane inhalation (2.5% in oxygen) delivered at 1.5 L/min (VetEquip, Piney River, VA). IOP of the right eyes was measured before injection and measured weekly after injection using a TonoLab tonometer (Colonial Medical Supply, Londonderry, NH), calculated as the average of three separate IOP determinations, each consisting of the mean of six error-free

readings. IOP was measured at a similar time of day to avoid diurnal fluctuations.[31]

Weigert's Resorcin Fuchsin Staining

Mice were sacrificed by CO_2 inhalation, followed by cervical dislocation and their eyes were enucleated and fixed in 4% paraformaldehyde (PFA) in PBS at room temperature for 24 hours. Eyes were dehydrated in gradient ethanol, embedded in paraffin, and then sectioned in the sagittal plane at 7-μm thickness using a cryostat (Leica, Deerfield, IL). Optic nerve cross-sections were taken proximal to the globe at the position of the glial lamina. Tissue sections were heated at 60°C for 20 minutes, then deparaffinized and rehydrated. Sections were oxidized in 10% fresh OXONE (catalog #228036; Sigma) for 30 minutes, and rinsed with H_2O, 70% and 95% ethanol. Slides were submerged in Weigert's resorcin fuchsin solution (Electron Microscopy Sciences, Hatfield, PA) for 1 hour and washed with 95% ethanol and H_2O. Nuclei were counterstained with 1:1 hematoxylin A and B. For sagittal eye sections, collagen was stained with Van Gieson's solution (Electron Microscopy Sciences) for 30 seconds and washed with H_2O. Sections were dehydrated, cleared with xylene, and mounted with Permount mounting medium (Fisher Scientific, Waltham, MA). Collagen was stained pink, and elastic fibers and elastin-free microfibrils were stained purple.

In Situ Hybridization

Mice were sacrificed by cervical dislocation and their eyes were enucleated and fixed in 4% PFA in PBS at room temperature for 24 hours. Eyes were embedded in paraffin and sectioned in the sagittal plane at a thickness of 7 μm using Leica cryostats. *In situ* hybridization was performed using the RNAscope technique (RNAscope 2.5 HD Chromogenic Assay-Red; Advanced Cell Diagnostics, Hayward, CA) following the manufacturer's instructions. Target probe sets were generated against Lox and Loxl1 transcripts, which include 20 different 50-bp nucleotides. Individual mRNA molecules were detected as red punctate dots. Target probes against *DapB*, a bacterial gene encoding dihydrodipicolinate reductase, and *Polr2a*, a gene encoding RNA polymerase II subunit A, were used as a negative and positive control, respectively. For each probe, several sections from at least three animals were examined.

Periodic Acid-Schiff Staining

Periodic acid-Schiff staining was shown to be capable of recognizing XFM in a previous study,[32] therefore, this method was chosen to investigate the presence of XFM in the eyes. A periodic acid-Schiff kit (catalog #395B; Sigma) was used following the manufacturer's instructions to stain the paraffin-fixed and sectioned eye specimens from WT and $Fbn1^{C1041G/+}$ mice injected with PBS and BAPN. Briefly, 7-μm–thick sections were deparaffinized in xylene and rehydrated in deionized water. Slides were immersed in periodic acid solution for 5 minutes at room temperature, rinsed with distilled water, immersed in Schiff's reagent for 15 minutes at room temperature, and washed in running tap water for 5 minutes. Sections were counterstained with Gill no. 3 hematoxylin solution for 90 seconds and rinsed in running tap water. Finally, sections were dehydrated in gradient ethanol and mounted using Permount mounting media. Brightfield images were acquired using a microscope equipped with a 20× objective (Nikon, Tokyo, Japan).

Immunohistochemistry

After euthanasia by CO_2 inhalation, mice were cardiac-perfused with PBS followed by 4% PFA in PBS. Eyes were enucleated and postfixed in 4% PFA in PBS for 1 hour, embedded in paraffin, and sectioned in the sagittal plane at a thickness of 7 μm. Central eye sections were deparaffinized, rehydrated, and blocked with 5% normal donkey serum for 2 hours at room temperature in a humid chamber. After blocking, sections were incubated with goat anti–microfibril-associated glycoprotein 1 polyclonal antibody (Santa Cruz Biotechnology, Dallas, TX) or rabbit anti–fibrillin-1 antibody (diluted 1:100, kindly provided by Dr. Lynn Sakai) at 4°C overnight. Microfibril-associated glycoprotein 1 co-localizes with fibrillin microfibrils, which ensheathe all elastic fibers. Microfibril-associated glycoprotein 1 was used as an indirect indicator of elastic fiber abundance, although elastin-free fibrillin-1 microfibrils also could be represented in the immunofluorescence signal. Sections were washed and then incubated with secondary antibody (Alexa Fluor 564–conjugated donkey anti-goat) diluted 1:1000 for 2 hours at room temperature. Sections then were incubated with DAPI working solution for 3 minutes, washed, and cover-slipped with mounting medium (Prolong Gold; Thermo Fisher Scientific, Waltham, MA).

Quantification of Optic Nerve and Pia Mater Size

After euthanasia by CO_2 inhalation, mice were cardiac-perfused with PBS followed by 4% PFA in PBS. Optic nerves were dissected and fixed in 1% glutaraldehyde/4% PFA in PBS for 24 to 48 hours, and then postfixed in 2% osmium for 1 hour. Samples were dehydrated in a graded ethanol series and infiltrated with Epon/araldite resin (Electron Microscopy Sciences) using propylene oxide as the transition solvent and the resin polymerized at 60°C for 48 hours.[22] Cross-sections of optic nerves were cut approximately 1.5 mm behind the globe with a thickness of 1 μm using an ultramicrotome (Leica) and stained with p-phenylenediamine. Images of optic nerves were acquired using an upright light microscope equipped with a 100× 1.45 numerical aperture oil immersion objective and a single-lens reflex camera (DS-Ri2; Nikon). Tiling images of the entire nerve cross-section were assembled in NIS-Elements (Nikon). Optic nerve area was determined in ImageJ (Fiji 2.9.0; NIH, Bethesda, MD; *https://imagej.net*) by drawing

polygons around the optic nerve, not including the pia mater. Axon area was determined by AxonJ (*https://imagej.net/ij/plugins/axonj/index.html*).[33] As previously described,[23] pia mater thickness was determined by measuring the area of the nerve including the pia mater (A_{total}) and the area of the nerve not including the pia mater (A_{inner}) using the polygon drawing function of ImageJ. The outer radius of the nerve including the pia mater (Ro) was calculated as equal to the square root of A_{total}/π and the inner radius not including the pia mater (Ri) was calculated as the square root of A_{inner}/π. Pia mater thickness then was calculated as Ro − Ri.

Transmission Electron Microscopy

Epon-embedded optic nerves that were used for axon quantification also were used for examining the ultrastructure of the elastic fibers. Cross-sections of optic nerves were cut approximately 1.5 mm behind the globe with a thickness of 70 nm using an ultramicrotome (Leica). Then they were collected onto 200 mesh nickel grids and stained with phosphotungstic acid,[34] followed by 2% uranyl acetate and lead citrate. Images of the pia mater region were acquired using Tecnai T-12 (Hillsboro, OR) transmission electron microscopy equipped with an AMT (Woburn, MA) complementary metal oxide semiconductor camera system. Images were captured at a magnification of ×4400 from the region of interest set in SerialEM acquisition software version 3.8.6 (*https://bio3d.colorado.edu/SerialEM/download.html*) and assembled using the IMOD software suite version 4.11.5 (*https://bio3d.colorado.edu/imod*).

Microfibril and Elastic Fiber Quantification

The abundance of microfibrils in the pia mater of each optic nerve was graded on a scale from 0 to 5 based on the appearance of microfibrils surrounding cross-sectional elastin cores, where 0 represents no observed microfibrils and 5 represents a high abundance of microfibrils. Examples are shown in Supplemental Figure S1.

The density of elastic fibers was determined in a masked fashion by counting elastic fiber units including cross-sectional, longitudinal, or oblique orientations in representative regions and dividing them by the area of the regions counted. Examples are shown in Supplemental Figure S2. The area of elastic fibers was measured by drawing masks around the electron-dense cores of individual cross-sectional elastic fibers.

Experimental Design and Data Analysis

A total of 28 WT and 30 *Fbn1*$^{C1041G/+}$ mice were assigned randomly to either the PBS- or BAPN-treated group. One mouse from the BAPN-treated *Fbn1*$^{C1041G/+}$ group died 7 weeks after injection, and thus tissues were not collected. Each optic nerve from the same mouse was considered independently. One optic nerve from the BAPN-treated WT group, two from the PBS-treated *Fbn1*$^{C1041G/+}$ group, and two from the BAPN-treated *Fbn1*$^{C1041G/+}$ group were lost during sample collection. The *t*-test was used for analysis. Data are presented as means ± SD.

Results

Lox and Loxl1 mRNA Expression in Ocular Tissue

The meninges tissue, including the dura mater and pia mater, ensheathe the optic nerve and are enriched in elastic fibers and collagen as seen by staining with Weigert's resorcin fuchsin, which stains elastic fibers purple, and with von Gieson's stain, which labels collagens pink (Figure 1, A and B). Expression of Lox and Loxl1 mRNA transcripts was examined in 9-month-old WT mice by *in situ* hybridization, which revealed Lox and Loxl1 mRNA transcripts within the pia mater and dura mater (Figure 1, C and D). In addition, Lox and Loxl1 mRNA transcripts were detected in the corneal stroma and endothelium, lens epithelial cells, nonpigmented ciliary epithelium, sclera, retina, and optic nerve (Supplemental Figures S3–S6). Loxl1 mRNA transcript was also detected in trabecular meshwork (Supplemental Figure S4). No mRNA signal was detected in sections incubated with the negative control probe (Figure 1E).

XFM Deposits Are Not Observed in the Eyes from BAPN-Treated *Fbn1*$^{C1041G/+}$ Mice

XFS is characterized by accumulation of XFM, predominantly consisting of LOXL1 and fibrillin-1, and deposited most prominently on the surfaces of the anterior lens capsule. By slit lamp examination of the anterior segment of eyes of living mice, no XFM deposits were detected (data not shown). Eye sections also were examined for XFM deposits by periodic acid-Schiff staining, which confirmed the lack of XFM detection (data not shown).

IOP Is Not Increased in BAPN-Treated *Fbn1*$^{C1041G/+}$ Mice

In XFG, accumulation of XFM in the anterior segment of the eye likely impedes outflow of aqueous humor, causing an increase in IOP.[4,35] IOP of WT and *Fbn1*$^{C1041G/+}$ mice was measured before commencement of daily intraperitoneal injections, then weekly for 8 weeks after daily injections began, using a TonoLab tonometer. IOP of WT and *Fbn1*$^{C1041G/+}$ mice did not change with either PBS or BAPN injection, compared with the baseline IOP (Figure 2) (paired *t*-test). Baseline IOP for *Fbn1*$^{C1041G/+}$ mice was significantly lower than that of WT mice (both $n = 29$, $P = 0.004$, data not shown). A similar trend was seen previously toward a lower IOP in mice with fibrillin-1 deficiency owing to the *Tsk* mutation of *Fbn1*.[22] A lack of increased IOP in BAPN-treated *Fbn1*$^{C1041G/+}$ mice is consistent with an absence of XFM deposits and suggests that the combined effects of the fibrillin-1 mutation and pan-

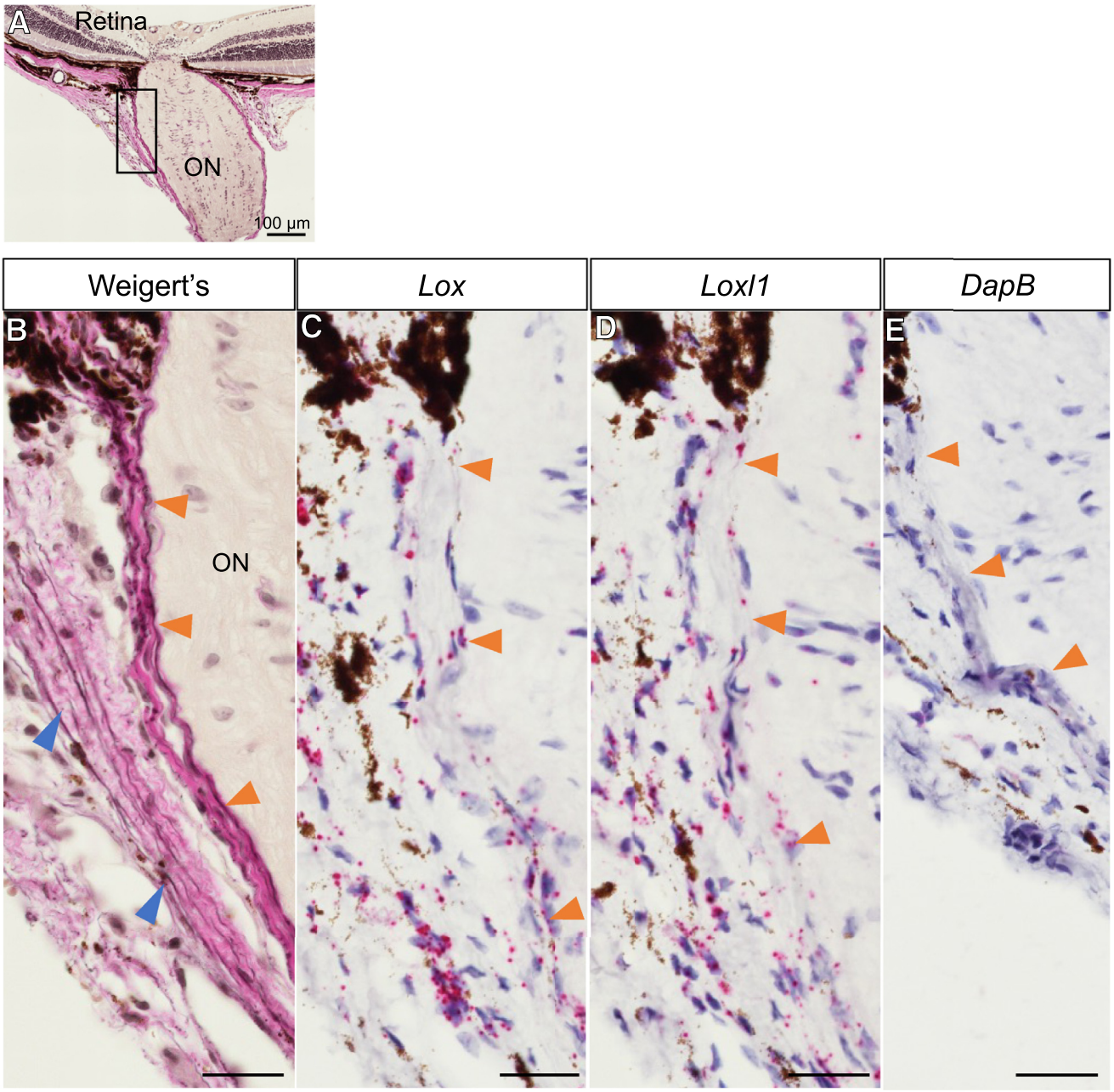

Figure 1 Lox and Loxl1 mRNA are expressed in the dura mater and pia mater of the mouse optic nerve. **A:** Weigert's resorcin fuchsin with van Gieson counterstain of the posterior segment of a sagittal eye section from a WT mouse at 9 months of age. **B:** Expanded view of the meningeal region outlined by the black rectangle in panel **A** showing elastic fibers stained purple and collagen stained pink. **C** and **D:** *In situ* hybridization analysis of adjacent sections showing that Lox and Loxl1 mRNA transcripts are expressed in the pia and dura mater, visible as **red dots**. **E:** No signal was detected from a bacterial gene, *DapB*, which served as the negative control. **C, D, and E:** Nuclei were counterstained with Gill's hematoxylin. **Orange arrowheads** indicate the pia mater, and **blue arrowheads** indicate the dura mater. Scale bars: 100 μm (**A**); 25 μm (**B**–**E**). ON, optic nerve.

LOX inhibition do not result in significant accumulation of XFM in the aqueous humor outflow of the eye.

Optic Nerve and Axon Expansion in BAPN-Treated *Fbn1*$^{C1041G/+}$ Mice

Tsk mutation results in the optic nerve expansion in mice with fibrillin-1 deficiency,[22] reminiscent of aorta dilation in *Fbn1*$^{C1041G/+}$ mice.[27] Herein, this was accompanied by thinning of the pia matter, the inner meningeal tissue that wraps tightly around the optic nerve. It was hypothesized that the thinner pia mater, which is rich in elastic fibers, was weakened biomechanically, allowing for the observed expansion. To determine whether a similar expansion of the optic nerve occurs in *Fbn1*$^{C1041G/+}$ mice and the effects of BAPN treatment on that expansion, the cross-sectional

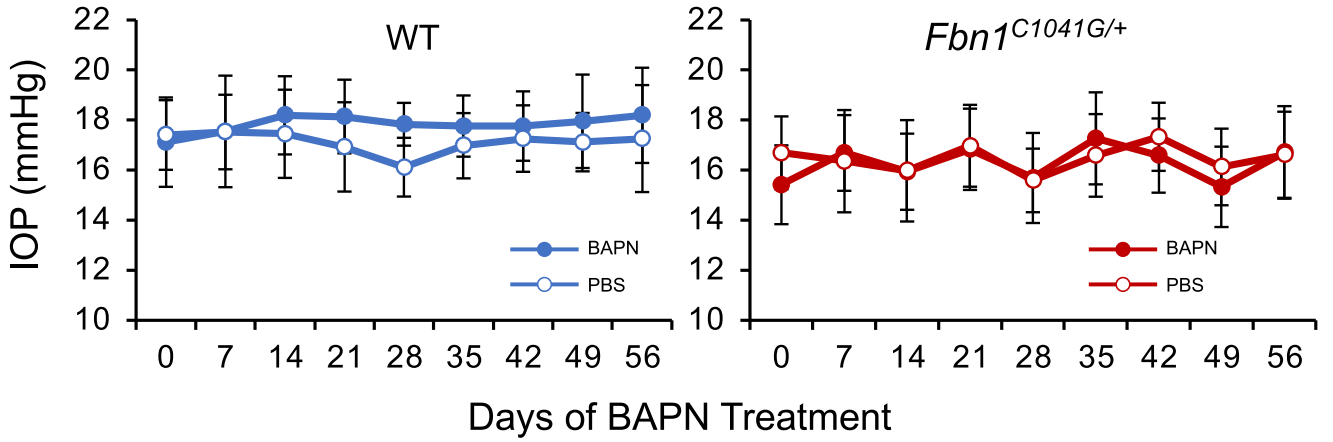

Figure 2 Increased intraocular pressure (IOP) does not change after β-aminopropionitrile (BAPN) treatment for either WT or *Fbn1*$^{C1041G/+}$ mice. IOP of the right eye was measured before treatment and once weekly for 8 weeks during the treatment period. IOP of WT mice and *Fbn1*$^{C1041G/+}$ mice was not changed with either phosphate-buffered saline (PBS) treatment (**open circles**) or BAPN treatment (**closed circles**), compared with the baseline IOP on day 0 of each group. $n = 29$ (**left panel**); $n = 29$ (**right panel**). $P = 0.004$, paired *t*-test.

area of the optic nerves was measured. After PBS treatment, *Fbn1*$^{C1041G/+}$ mice had larger optic nerves compared with WT (Figure 3A) ($P = 0.003$, t-test), consistent with previous findings of expanded optic nerves resulting from fibrillin-1 deficiency. BAPN induced further expansion of the optic nerve in *Fbn1*$^{C1041G/+}$ mice compared with PBS (Figure 3A) (0.110 ± 0.011 versus 0.104 ± 0.009 mm^2; $n = 30$ and 24, respectively; $P = 0.03$), but did not expand the optic nerve in WT mice compared with PBS (Figure 3A) (0.098 ± 0.010 versus 0.098 ± 0.007 mm^2; $n = 27$ and 28, respectively; $P = 0.94$).

Axon enlargement also accompanies expansion of the optic nerve in mice with the *Tsk* mutation of *Fbn1*.[22] Similarly, PBS-treated *Fbn1*$^{C1041G/+}$ mice had larger optic nerve axons compared with WT mice (Figure 3B) ($P = 0.002$). As with the optic nerve, BAPN-treated *Fbn1*$^{C1041G/+}$ mice displayed further expansion of optic nerve axons compared with PBS-treated *Fbn1*$^{C1041G/+}$ mice (Figure 3B) (0.661 ± 0.048 versus 0.635 ± 0.036 μm^2;

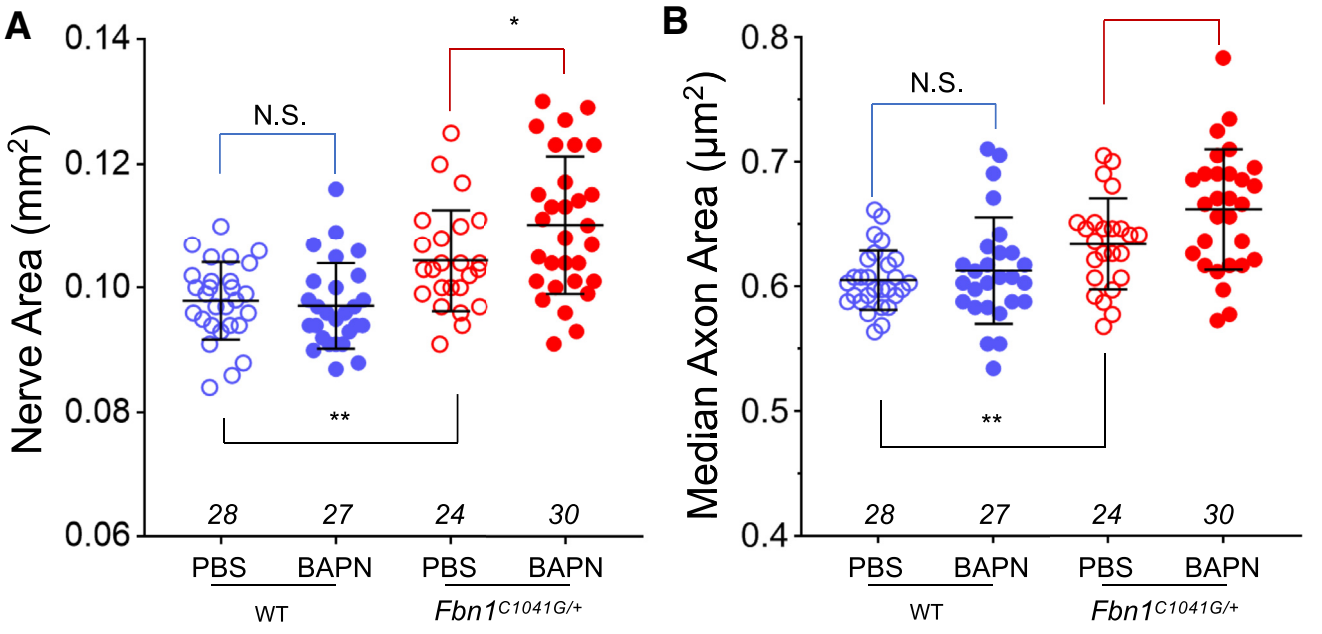

Figure 3 **A** and **B:** Expansion of optic nerves (**A**) and optic nerve axons (**B**). For phosphate-buffered saline (PBS)-treated mice, the optic nerve area and the median optic nerve axon area was larger in *Fbn1*$^{C1041G/+}$ mice (**red open symbols**) compared with WT mice (**blue open symbols**). Optic nerves and optic nerve axons were expanded in β-aminopropionitrile (BAPN)-treated *Fbn1*$^{C1041G/+}$ mice (**red closed symbols**) compared with *Fbn1*$^{C1041G/+}$ mice treated with PBS (**red open symbols**). BAPN did not affect optic nerve or axon size of WT mice (**blue symbols**). $n = 28$ (**blue open symbols**); $n = 27$ (**blue closed symbols**); $n = 24$ (**red open symbols**); $n = 30$ (**red closed symbols**). *$P < 0.05$, **$P < 0.01$. N.S., nonsignificant.

$P = 0.03$). PBS treatment did not induce any axon size changes in WT mice (Figure 3B) (0.613 ± 0.043 versus 0.605 ± 0.024 μm^2; $P = 0.43$). These results show that when combined with fibrillin-1 deficiency, inhibition of lysyl oxidases exerts an expansive effect on the optic nerve and its axons.

Thinner Optic Nerve Pia Mater and Smaller Pia Area in *Fbn1*$^{C1041G/+}$ Mice

Thinning of the pia mater in mice carrying the *Tsk* mutation of *Fbn1* was hypothesized to be weakened and could allow optic nerve expansion.[22] In this study, PBS treatment in the *C1041G* mutation of *Fbn1* mice resulted in a similar effect, with 43% thinner pia mater compared with that in WT (2.53 ± 0.65 μm versus 3.62 ± 0.71 μm; $P = 0.00004$) (Figure 4A). The area of the pia mater was also reduced (Figure 4B), suggesting tissue remodeling rather than simple stretching of existing pia mater tissue to accommodate optic nerve enlargement. After BAPN administration, pia mater thickness did not change significantly in either WT or *Fbn1*$^{C1041G/+}$ mice, suggesting that the further expansion of the optic nerve seen in BAPN-treated *Fbn1*$^{C1041G/+}$ mice (Figure 4A) was not the result of a further thinning of the pia mater.

Morphologic Changes of Elastic Fibers in the Optic Nerve Pia Mater of BAPN-Treated *Fbn1*$^{C1041G/+}$ Mice

BAPN treatment of *Fbn1*$^{C1041G/+}$ mice exacerbates elastic fiber defects in the wall of the aorta.[27] To determine whether BAPN altered elastic fibers in the pia mater, optic nerve cross-sections were stained with Weigert's resorcin fuchsin and imaged by light microscopy. Elastic fibers in the pia mater are oriented either longitudinally, running parallel to the long axis of the optic nerve, or circumferentially around the optic nerve.[36] The inner region of the pia mater adjacent to the optic nerve contains primarily longitudinal elastic fibers, whereas the elastic fibers in the outer pia mater are oriented circumferentially.[36] In the optic nerve cross-sections, longitudinal elastic fibers were cross-sectioned and appear as dots, whereas circumferential elastic fibers encircle the nerve as shown for PBS-treated WT mice (Figure 5A). Longitudinal elastic fibers were distributed somewhat evenly in WT mice (Figure 5A), whereas in *Fbn1*$^{C1041G/+}$ mice they mostly were distributed irregularly and formed disorganized structures (Figure 5E). BAPN treatment in combination with the *Fbn1* mutation induced significantly noticeable changes of elastic fiber morphology in some areas of the pia mater, with dots distributed extensively in both inner and outer layers of pia mater (Figure 5G) that were seen infrequently in the WT cohorts (Figure 5C).

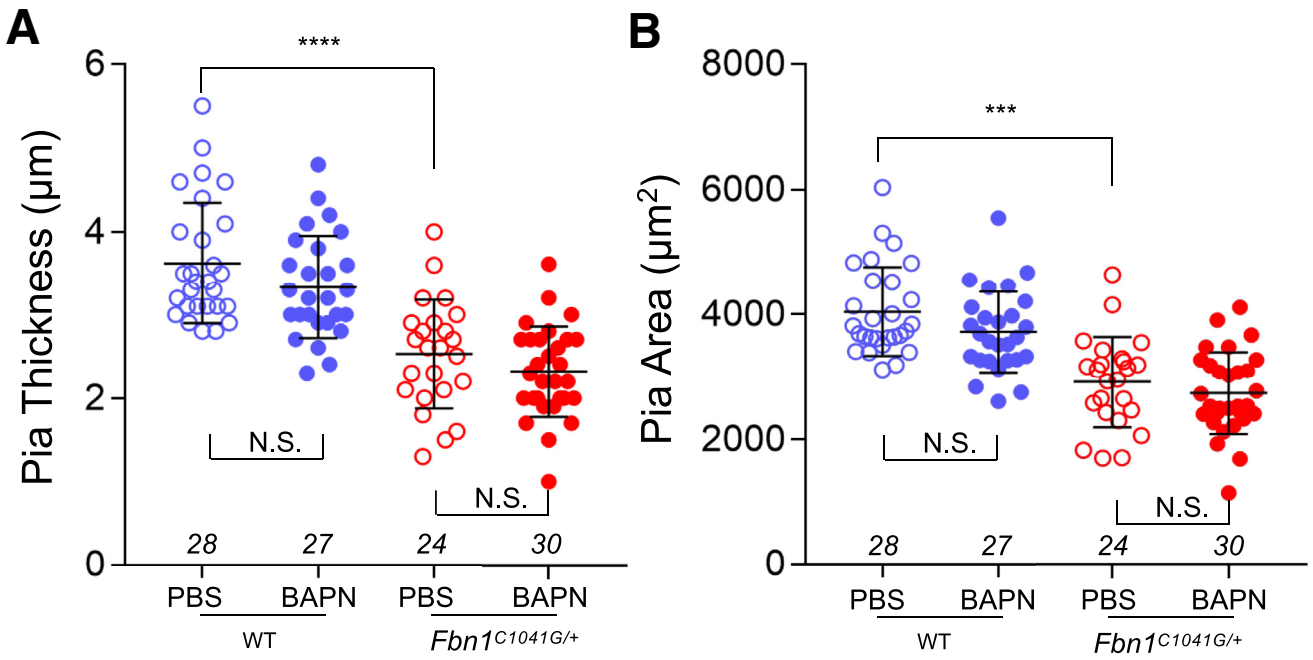

Figure 4 Smaller pia mater area and thinner pia mater in *Fbn1*$^{C1041G/+}$ mice. **A:** Compared with phosphate-buffered saline (PBS)-treated WT mice, PBS-treated *Fbn1*$^{C1041G/+}$ mice have thinner pia mater. Pia mater thickness was not changed in either WT or *Fbn1*$^{C1041G/+}$ mice after β-aminopropionitrile (BAPN) treatment compared with corresponding PBS-treated WT or *Fbn1*$^{C1041G/+}$ mice. **B:** Compared with the PBS-treated WT mice, PBS-treated *Fbn1*$^{C1041G/+}$ mice had a smaller pia mater area. The pia mater area was not changed in either WT or *Fbn1*$^{C1041G/+}$ mice after BAPN treatment compared with corresponding PBS-treated WT or *Fbn1*$^{C1041G/+}$ mice. $n = 28$ (PBS-treated WT mice); $n = 24$ (PBS-treated *Fbn1*$^{C1041G/+}$ mice); $n = 27$ (WT mice after BAPN treatment); $n = 30$ (*Fbn1*$^{C1041G/+}$ mice after BAPN treatment). ***$P < 0.001$, ****$P < 0.0001$. N.S., nonsignificant.

Immunohistochemistry staining of pia mater using antibody against microfibril-associated glycoprotein 1, which has been shown as an integral component of elastic fibers,[37] led to easy recognition of the morphologically differential staining of the inner and outer layers of pia mater in WT mice treated with PBS (Figure 5B). While the distribution and intensity were maintained by BAPN treatment (Figure 5D), the alterations in *Fbn1*$^{C1041G/+}$ mice treated with PBS and BAPN were easily detectable (Figure 5, F and H), especially with BAPN treatment. These findings are consistent with histologic changes demonstrated by Weigert's resorcin fuchsin staining.

Altered Ultrastructure of Elastic Fibers in the Optic Nerve Pia Mater of BAPN-Treated *Fbn1*$^{C1041G/+}$ Mice

To examine the ultrastructure of elastic fibers in the pia mater, optic nerves were cross-sectioned, stained with phosphotungstic acid,[34] uranyl acetate, and lead citrate, and imaged by transmission electron microscopy. Regions of the

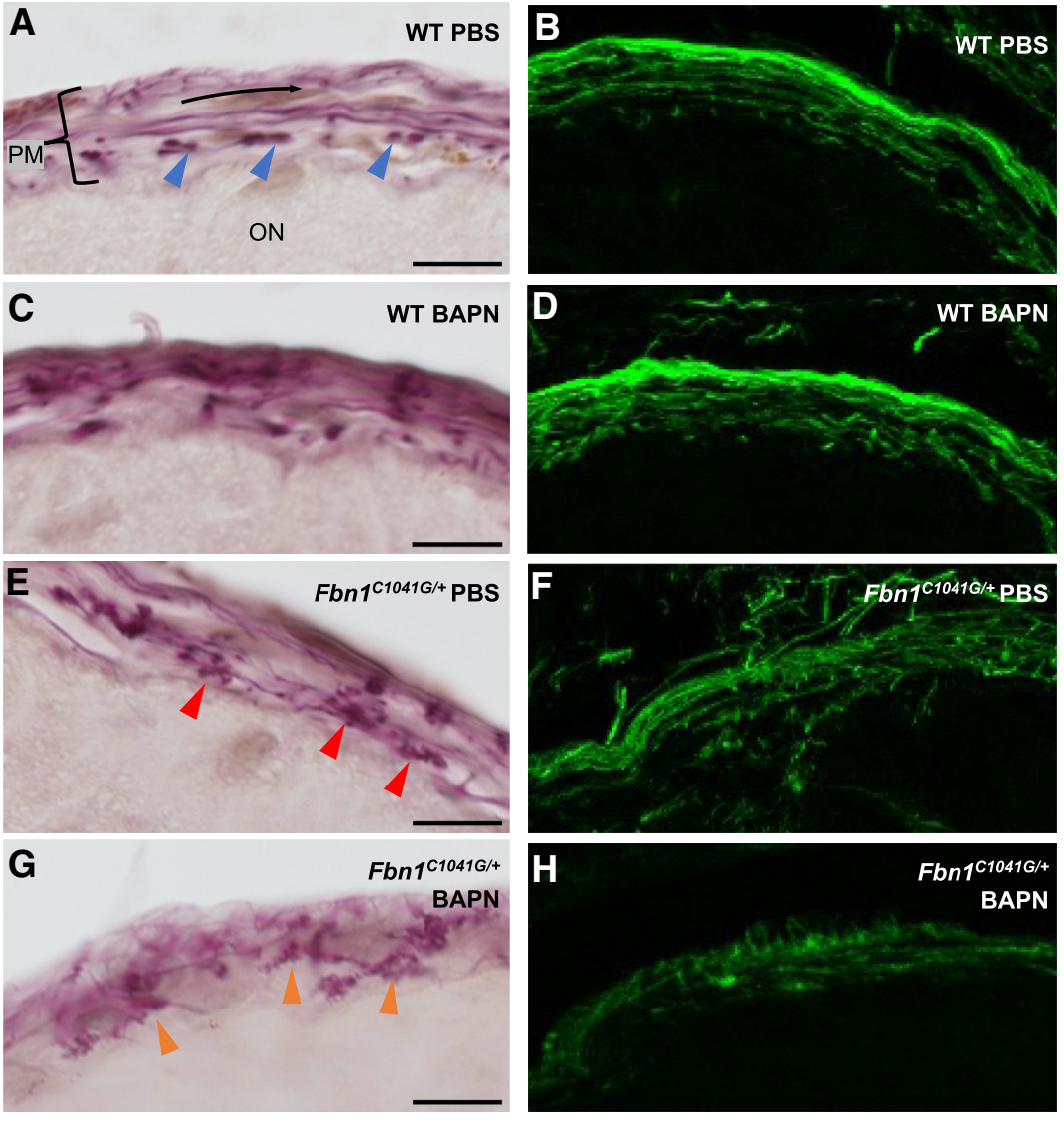

Figure 5 Morphologic changes of elastic fibers in the optic nerve (ON) pia mater (PM) of *Fbn1*$^{C1041G/+}$ mice. **A:** Cross-sections of the optic nerve stained with Weigert's resorcin fuchsin show elastic fibers within the pia mater (**bracket**) oriented either longitudinally, appearing as regularly distributed purple dots (**blue arrowheads**), or circumferentially as purple fibers (**black arrow**). **A** and **C:** The pia mater of β-aminopropionitrile (BAPN)-treated WT mice (**C**) was similar to phosphate-buffered saline (PBS)-treated WT mice (**A**). **E:** *Fbn1*$^{C1041G/+}$ mice commonly displayed disorganized elastic fibers distributed irregularly (**red arrowheads**). **G:** For BAPN-treated *Fbn1*$^{C1041G/+}$ mice, some regions of the pia mater displayed increased disorganization of elastic fibers (**orange arrowheads**), which can be appreciated further with immunohistochemistry staining of pia mater using antibody against microfibril-associated glycoprotein 1. **B** and **D:** Differential staining of inner and outer layers of elastic fiber is seen in the pia mater of WT mice (**B**), which largely is preserved in WT mice treated with BAPN (**D**). **F** and **H:** However, disorganized elastic fibers are seen in pia mater of *Fbn1*$^{C1041G/+}$ mice (**F**), which is affected further in *Fbn1*$^{C1041G/+}$ mice treated with BAPN (**H**). $n = 9$ (PBS-injected WT mice); $n = 7$ (BAPN-injected WT mice); $n = 7$ (PBS-injected *Fbn1*$^{C1041G/+}$ mice); $n = 10$ (BAPN-injected *Fbn1*$^{C1041G/+}$ mice). Scale bars = 20 μm.

pia mater were selected randomly for imaging, avoiding the ophthalmic artery. Elastic fibers were identified morphologically as having electron-dense cores ensheathed by microfibrils.[34] Longitudinal elastic fibers appear as cross-sectioned whereas radial elastic fibers appear as sectioned along their long axis.

The apparent abundance of microfibrils surrounding cross-sectional elastic cores was graded from 0 to 5, where 0 corresponds to almost no microfibrils and 5 represents extensive microfibrils (Supplemental Figure S1). The pia mater of *Fbn1*$^{C1041G/+}$ mice had a significantly lower apparent abundance of microfibrils compared with WT mice, as can be seen in representative images (Figure 6, A and C) and quantitation (Figure 6E). However, BAPN treatment did not affect microfibril abundance in either WT or *Fbn1*$^{C1041G/+}$ mice (Figure 6, B, D, and E).

The size of elastic fibers in the pia mater was investigated by measuring the area of the electron-dense cores of cross-sectional elastic fibers. *Fbn1*$^{C1041G/+}$ mice displayed significantly smaller elastic fibers compared with WT mice (Figure 6F). BAPN treatment significantly expanded the cross-sectional elastin area in both WT and *Fbn1*$^{C1041G/+}$ mice (Figure 6F).

The density of elastic fibers in the pia mater was determined by counting cross-sectional and longitudinal elastic fiber units (Supplemental Figure S2), divided by the area analyzed. In *Fbn1*$^{C1041G/+}$ mice, elastic fiber density was reduced significantly compared with WT mice (Figure 6G). Elastic fiber density increased in response to BAPN

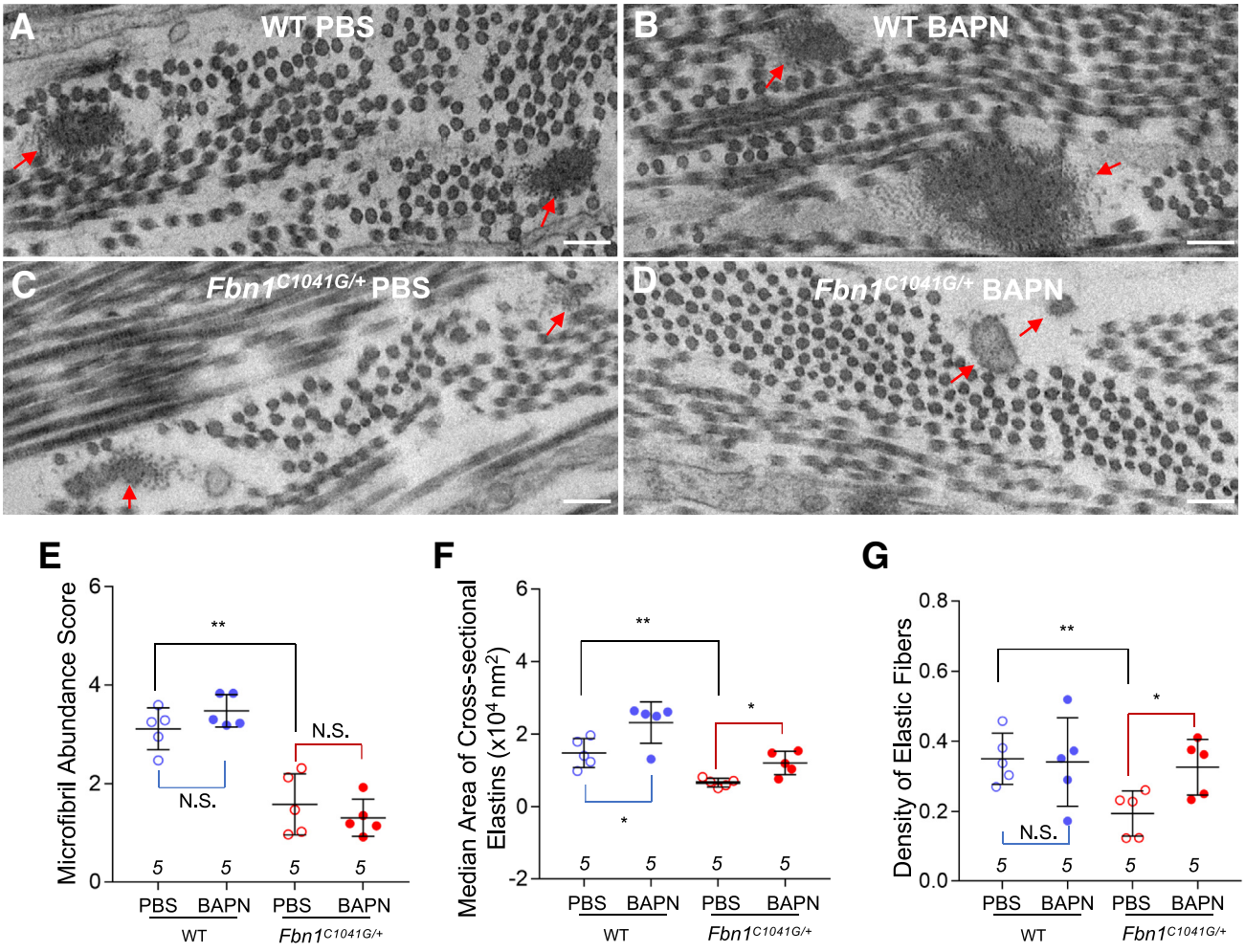

Figure 6 Ultrastructural changes of elastic fibers in the optic nerve pia mater. **A**—**D:** Representative transmission electron microscopy images of elastic fibers (**red arrows**) in the pia mater of the optic nerve from WT or *Fbn1*$^{C1041G/+}$ mice treated with either phosphate-buffered saline (PBS) or β-aminopropionitrile (BAPN). Pia mater regions that were quantified for the elastic fiber parameters count for approximately 10% of the total pia mater area for each optic nerve sample. Samples from five mice from each group were quantified. **E:** The apparent abundance of microfibrils associated with cross-sectional elastin cores was lower for *Fbn1*$^{C1041G/+}$ mice compared with WT, but was not affected by BAPN treatment. **F:** Median cross-sectional area of elastin cores was lower for *Fbn1*$^{C1041G/+}$ mice compared with WT, and increased with BAPN treatment for both WT and *Fbn1*$^{C1041G/+}$ mice. **G:** For *Fbn1*$^{C1041G/+}$ mice, the density of elastic fiber units was lower compared with WT. BAPN increased elastic fiber density for *Fbn1*$^{C1041G/+}$ mice, but not for WT mice. WT mice injected with PBS (**blue open symbols**), WT mice injected with BAPN (**blue closed symbols**), *Fbn1*$^{C1041G/+}$ mice injected with PBS (**red open symbols**), and *Fbn1*$^{C1041G/+}$ mice injected with BAPN (**red closed symbols**) are shown. $^{*}P < 0.05$, $^{**}P < 0.01$. Scale bars: 200 nm. N.S., nonsignificant.

treatment of *Fbn1*$^{C1041G/+}$ mice, but was not affected by BAPN treatment of WT mice (Figure 6G).

Discussion

The present study characterized ocular phenotypes of mice with combined microfibril deficiency and pan-LOX inhibition. Although XFM deposits were not found in ocular tissues, LOX inhibition in microfibril-deficient mice led to enhanced optic nerve and axon expansion, and alteration of elastic fiber structures in the pia mater of the optic nerve as demonstrated by histologic and immunohistochemistry staining, as well as transmission electron microscopy. As the first gene identified to be associated with XFS and XFG,[9] the role of *LOXL1* in disease pathogenesis has been investigated extensively via tissues and cultured cells from patients with XFG or animal models that either lack or overexpress *LOXL1*.[16,38–40] Yet, the precise role of *LOXL1* in disease pathogenesis remains elusive.

In humans, mRNA and protein expression of LOX family members is well documented in various ocular tissues such as cornea, iris, lens, ciliary body, retina, lamina cribrosa, and optic nerve.[2,41,42] Here, ubiquitous expression of Lox and Loxl1 mRNA in mouse ocular tissues by *in situ* hybridization (Figure 1 and Supplemental Figures S3–S6) is reported, which was similar to humans, except that mice do not have lamina cribrosa and the expression levels in the optic nerve are relatively low compared with the optic nerve pia mater. In human optic nerves, *LOXL1* has higher mRNA expression compared with LOX and LOXL2, and is the dominant LOX isoform in the normal lamina cribrosa associated with a complex extracellular matrix network,[5] suggesting that LOXL1 is the dominant LOX isoform in the optic nerve. Functional dominance of LOX family members has been reported in the setting of other diseases. For example, in animal models of idiopathic pulmonary fibrosis, LOXL4 functions as the critical determinant for collagen cross-linking and fibrosis.[43]

Loxl1 mRNA was also expressed in the aqueous humor outflow apparatus (Supplemental Figure S4). A balance between aqueous humor production and drainage determines IOP. Extracellular matrix of the juxtacanalicular tissue region of the trabecular meshwork and the inner wall basement membrane of Schlemm's canal are thought to provide the most aqueous outflow resistance.[44] Elastic fibers are expressed extensively in the juxtacanalicular tissue region of the trabecular meshwork and within the collector channel wall of human eyes,[45] suggesting a role in generating outflow resistance. However, the IOP was not increased in either WT or *Fbn1*$^{C1041G/+}$ mice treated with BAPN. On the other hand, because XFM deposits were not detected in the anterior segment of the eyes from LOX-inhibited microfibril-deficient mice, there was no expectation that a change in IOP would be observed. Interestingly, focusing on LOXL1 alone, conflicting IOP data have been reported for *Loxl1*$^{-/-}$ mice.[16,38,39] Li et al[39] reported an increased IOP in *Loxl1*$^{-/-}$ mice that was associated paradoxically with increased outflow facility. The role of LOXL1 in conventional outflow function needs to be explored further.

Although the IOP was not changed, accelerated optic nerve and RGC axon expansion in BAPN-treated *Fbn1*$^{C1041G/+}$ mice was observed (Figure 3). In the absence of BAPN treatment, *Fbn1*$^{C1041G/+}$ mice have enlarged optic nerves and RGC axons compared with WT. This is consistent with the previous findings of expanded optic nerves in another microfibril-deficient mouse line, *Fbn1*$^{Tsk/+}$.[22] Fibrillin 1 is expressed in pia mater of the optic nerve, but was reduced in *Fbn1*$^{C1041G/+}$ mice as shown in Supplemental Figure S7. In both *Fbn1*$^{Tsk/+}$ as shown previously and in *Fbn1*$^{C1041G/+}$ mice in the current study, optic nerve expansion is associated with thinning of the optic nerve pia mater (Figure 4), suggesting that microfibril defects affect the integrity of the pia mater. Furthermore, accelerated optic nerve expansion occurred only in BAPN-treated *Fbn1*$^{C1041G/+}$ mice, but not in WT groups, likely owing to further worsening of optic nerve pia mater induced by LOX inhibition. Consistent with this notion, disorganized elastic fibers were found to be increased in BAPN-treated *Fbn1*$^{C1041G/+}$ mice (Figure 5), suggesting an exaggerated structural defect of elastic fiber in the context of microfibril deficiency and LOX inhibition.

To further investigate pia mater on the ultrastructural level, transmission electron microscopy was used, which showed that *Fbn1*$^{C1041G/+}$ mice had fewer fibrillin microfibrils, smaller elastin cores, and reduced density of elastic fibers in the optic nerve pia mater, further supporting that fibrillin microfibril is a prerequisite for elastic fiber formation. BAPN treatment led to elastin expansion in both WT and *Fbn1*$^{C1041G/+}$ mice, as reflected by an increased cross-sectional area of elastin in the optic nerve pia mater (Figure 6F), suggesting that constant cross-linking is required for maintaining the elastin core structure. The turnover rate of elastic fibers in *Fbn1*$^{C1041G/+}$ mice may be higher than normal because of defective microfibrils, therefore increased LOX activity is needed to counter the effects of microfibril deficiency. This notion is consistent with a previous report that Loxl1 mRNA is increased in the aorta of *Fbn1*$^{C1041G/+}$ mice.[27] Here, focusing on optic nerve pia mater, higher signals of both Lox and Loxl1 mRNA also were observed (Supplemental Figure S8). When the ongoing protective effect of elastic fiber cross-linking exerted by LOX and LOXL1 counteracting microfibril deficiency is inhibited, further pathology in the aorta and optic nerve ensue.

Increased density of elastic fibers was observed with BAPN treatment in the optic nerve pia mater from *Fbn1*$^{C1041G/+}$ mice (Figure 6G). This finding is counterintuitive. It is noteworthy that the expanded elastin core induced by BAPN treatment appears less electron-dense and fuzzy, suggesting reduced elastin cross-linking. In primary

cultured human optic nerve head astrocytes, elastin, but not fibrillin-1 or fibulin immunofluorescence, was decreased markedly with the addition of BAPN to transforming growth factor β1–stimulated cells, suggesting that inhibition of LOX interfered with elastin assembly.[5] Here, the possible explanation of the finding of increased density of elastic fibers in microfibril-deficient mice when treated with BAPN was speculated. LOX inhibition is likely to affect existing elastic fibers, whether it functioned normally in WT or was weakened in microfibril-deficient mice. LOX inhibition may accelerate the breaking down of weakened elastic fibers by elastase[46] in microfibril-deficient mice, reflected as significantly thinner optic nerve pia mater in *Fbn1*$^{C1041G/+}$ mice when compared with WT mice (Figure 4A). The enhanced disrupted elastic fibers revealed by both histologic and immunohistochemistry investigations of pia mater of *Fbn1*$^{C1041G/+}$ mice treated with BAPN supports this notion. The disruption of elastic fibers likely leads to increased density, as shown here. This is consistent with the previous report that significant elastic fiber fragmentation was observed in the aorta of *Fbn1*$^{C1041G/+}$ mice when treated with BAPN.[27] In addition, both the current and the Busnadiego et al[27] studies indicated increased Lox and Loxl1 mRNA in optic nerve pia mater (Supplemental Figure S7), and in the aorta wall of *Fbn1*$^{C1041G/+}$ mice.

It is important to note that the anatomy of the rodent optic nerve head, to some degree, is different from that of the human and nonhuman primate.[47] Quigley et al[48] reported loose microfibrils and curved elastic fibers in lamina cribrosa from patients with glaucoma and a nonhuman primate experimental model of glaucoma, suggesting that elastic fiber pathology is associated with glaucoma. Unlike humans, mice do not have lamina cribrosa, instead, they have glial lamina that is free of elastic fibers and collagens. In the microfibril-deficient mice, LOX inhibition worsened the enlargement of the optic nerve and optic nerve axons, which precedes axon loss in other rodent glaucoma models.[25] Presumably, humans would have more severe optic nerve phenotypes with inhibited LOXL1 activity because the lamina cribrosa is enriched in elastic fibers[48] and is thought to be the initial site of glaucomatous damage.[6–8]

This study was not without limitations. It focused primarily on morphologic changes of the optic nerve in the event of a combination of microfibril deficiency and LOX inhibition. In addition, the roles for individual LOX family members could not be defined because the pan-LOX inhibitor, BAPN, was used. The observation of enhanced optic nerve and axon expansion in *Fbn1*$^{C1041G/+}$ mice treated with BAPN provides the premise for further investigating the roles of fibrillin-1 and LOXL1 in XFG. For this, a mouse line with *Loxl1* knockout and *Fbn1*$^{C1041G/+}$ mutation was generated. The new mouse model should reveal specific interactions between fibrillin-1 and LOXL1, and, likely, in turn, XFG pathogenesis.

Disclosure Statement

None declared.

Supplemental Data

Supplemental material for this article can be found at *http://doi.org/10.1016/j.ajpath.2024.03.002*.

References

1. Schlötzer-Schrehardt U, Khor CC: Pseudoexfoliation syndrome and glaucoma: from genes to disease mechanisms. Curr Opin Ophthalmol 2021, 32:118–128
2. Schlötzer-Schrehardt U, Pasutto F, Sommer P, Hornstra I, Kruse FE, Naumann GOH, Reis A, Zenkel M: Genotype-correlated expression of lysyl oxidase-like 1 in ocular tissues of patients with pseudoexfoliation syndrome/glaucoma and normal patients. Am J Pathol 2008, 173:1724–1735
3. Schlötzer-Schrehardt U, Naumann GOH: Ocular and systemic pseudoexfoliation syndrome. Am J Ophthalmol 2006, 141:921–937.e2
4. Ritch R, Schlötzer-Schrehardt U, Konstas AG: Why is glaucoma associated with exfoliation syndrome? Prog Retin Eye Res 2003, 22: 253–275
5. Schlötzer-Schrehardt U, Hammer CM, Krysta AW, Hofmann-Rummelt C, Pasutto F, Sasaki T, Kruse FE, Zenkel M: Microfibril, prerequisite, elastic fiber formation. Ophthalmology 2012, 119: 1832–1843
6. Levy NS, Crapps EE: Displacement of optic nerve head in response to short-term intraocular pressure elevation in human eyes. Arch Ophthalmol 1984, 102:782–786
7. Yan DB, Coloma FM, Metheetrairut A, Trope GE, Heathcote JG, Ethier CR: Deformation of the lamina cribrosa by elevated intraocular pressure. Br J Ophthalmol 1994, 78:643–648
8. Bellezza AJ, Rintalan CJ, Thompson HW, Downs JC, Hart RT, Burgoyne CF: Deformation of the lamina cribrosa and anterior scleral canal wall in early experimental glaucoma. Invest Ophthalmol Vis Sci 2003, 44:623–637
9. Thorleifsson G, Magnusson KP, Sulem P, Walters GB, Gudbjartsson DF, Stefansson H, Jonsson T, Jonasdottir A, Jonasdottir A, Stefansdottir G, Masson G, Hardarson GA, Petursson H, Arnarsson A, Motallebipour M, Wallerman O, Wadelius C, Gulcher JR, Thorsteinsdottir U, Kong A, Jonasson F, Stefansson K: Common sequence variants in the LOXL1 gene confer susceptibility to exfoliation glaucoma. Science 2007, 317:1397–1400
10. Aung T, Ozaki M, Lee MC, Schlötzer-Schrehardt U, Thorleifsson G, Mizoguchi T, et al: Genetic association study of exfoliation syndrome identifies a protective rare variant at LOXL1 and five new susceptibility loci. Nat Genet 2017, 49:993–1004
11. Kagan HM, Li W: Lysyl oxidase: properties, specificity, and biological roles inside and outside of the cell. J Cell Biochem 2003, 88: 660–672
12. Liu X, Zhao Y, Gao J, Pawlyk B, Starcher B, Spencer JA, Yanagisawa H, Zuo J, Li T: Elastic fiber homeostasis requires lysyl oxidase–like 1 protein. Nat Genet 2004, 36:178–182
13. Baldwin AK, Simpson A, Steer R, Cain SA, Kielty CM: Elastic fibres in health and disease. Expert Rev Mol Med 2013, 15:e8
14. Judge DP, Dietz HC: Marfan's syndrome. Lancet 2005, 366: 1965–1976
15. Kim Y, Peyrol S, So C-K, Boyd CD, Csiszar K: Coexpression of the lysyl oxidase-like gene (LOXL) and the gene encoding type III procollagen in induced liver fibrosis. J Cell Biochem 1999, 72: 181–188

16. Wareham LK, Kuchtey J, Wu H-J, Krystofiak E, Wu Y, Reinhart-King CA, Kuchtey RW: Lysyl oxidase-like 1 deficiency alters ultrastructural and biomechanical properties of the peripapillary sclera in mice. Matrix Biol 2022, 16:100120
17. Ovodenko B, Rostagno A, Neubert TA, Shetty V, Thomas S, Yang A, Liebmann J, Ghiso J, Ritch R: Proteomic analysis of exfoliation deposits. Invest Ophthalmol Vis Sci 2007, 48:1447−1457
18. Sharma S, Chataway T, Burdon KP, Jonavicius L, Klebe S, Hewitt AW, Mills RA, Craig JE: Identification of LOXL1 protein and apolipoprotein E as components of surgically isolated pseudoexfoliation material by direct mass spectrometry. Exp Eye Res 2009, 89: 479−485
19. Creasey R, Sharma S, Gibson CT, Craig JE, Ebner A, Becker T, Hinterdorfer P, Voelcker NH: Atomic force microscopy-based antibody recognition imaging of proteins in the pathological deposits in pseudoexfoliation syndrome. Ultramicroscopy 2011, 111:1055−1061
20. Ronci M, Sharma S, Martin S, Craig JE, Voelcker NH: MALDI MS imaging analysis of apolipoprotein E and lysyl oxidase-like 1 in human lens capsules affected by pseudoexfoliation syndrome. J Proteomics 2013, 82:27−34
21. De Maria A, Zientek KD, David LL, Wilmarth PA, Bhorade AM, Harocopos GJ, Huang AJW, Hong AR, Siegfried CJ, Tsai LM, Sheybani A, Bassnett S: Compositional analysis of extracellular aggregates in the eyes of patients with exfoliation syndrome and exfoliation glaucoma. Invest Ophthalmol Vis Sci 2021, 62:27
22. Wu H-J, Hazlewood RJ, Kuchtey J, Kuchtey RW: Enlarged optic nerve axons and reduced visual function in mice with defective microfibrils. eNeuro 2018, 5:ENEURO.0260-18.2018
23. Wu H-J, Kuchtey J, Kuchtey RW: Increased susceptibility to glaucomatous damage in microfibril deficient mice. Invest Ophthalmol Vis Sci 2020, 61:28
24. Pazos M, Yang H, Gardiner SK, Cepurna WO, Johnson EC, Morrison JC, Burgoyne CF: Expansions of the neurovascular scleral canal and contained optic nerve occur early in the hypertonic saline rat experimental glaucoma model. Exp Eye Res 2016, 145:173−186
25. Cooper ML, Crish SD, Inman DM, Horner PJ, Calkins DJ: Early astrocyte redistribution in the optic nerve precedes axonopathy in the DBA/2J mouse model of glaucoma. Exp Eye Res 2016, 150:22−33
26. Judge DP, Biery NJ, Keene DR, Geubtner J, Myers L, Huso DL, Sakai LY, Dietz HC: Evidence for a critical contribution of haploinsufficiency in the complex pathogenesis of Marfan syndrome. J Clin Invest 2004, 114:172−181
27. Busnadiego O, Gorbenko del Blanco D, González-Santamaría J, Habashi JP, Calderon JF, Sandoval P, Bedja D, Guinea-Viniegra J, Lopez-Cabrera M, Rosell-Garcia T, Snabel JM, Hanemaaijer R, Forteza A, Dietz HC, Egea G, Rodriguez-Pascual F: Elevated expression levels of lysyl oxidases protect against aortic aneurysm progression in Marfan syndrome. J Mol Cell Cardiol 2015, 85:48−57
28. Ritch R, Schlötzer-Schrehardt U: Exfoliation syndrome. Surv Ophthalmol 2001, 45:265−315
29. De Maria A, Wilmarth PA, David LL, Bassnett S: Proteomic analysis of the bovine and human ciliary zonule. Invest Ophthalmol Vis Sci 2017, 58:573−585
30. Wilmarth KR, Froines JR: In vitro and in vivo inhibition of lysyl oxidase byaminopropionitriles. J Toxicol Environ Health 1992, 37: 411−423
31. Aihara M, Lindsey JD, Weinreb RN: Twenty-four-hour pattern of mouse intraocular pressure. Exp Eye Res 2003, 77:681−686
32. Yuan Y, Schlötzer-Schrehardt U, Ritch R, Call M, Chu FB, Dong F, Rice T, Zhang J, Kao WW-Y: Transient expression of Wnt5a elicits ocular features of pseudoexfoliation syndrome in mice. PLoS One 2019, 14:e0212569
33. Zarei K, Scheetz TE, Christopher M, Miller K, Hedberg-Buenz A, Tandon A, Anderson MG, Fingert JH, Abràmoff MD: Automated axon counting in rodent optic nerve sections with AxonJ. Sci Rep 2016, 6:26559
34. Greenlee TK, Ross R, Hartman JL: The fine structure of elastic fibers. J Cell Biol 1966, 30:59−71
35. Gottanka J, Flügel-Koch C, Martus P, Johnson DH, Lütjen-Drecoll E: Correlation of pseudoexfoliative material and optic nerve damage in pseudoexfoliation syndrome. Invest Ophthalmol Vis Sci 1997, 38: 2435−2446
36. Gelman S, Cone FE, Pease ME, Nguyen TD, Myers K, Quigley HA: The presence and distribution of elastin in the posterior and retrobulbar regions of the mouse eye. Exp Eye Res 2010, 90:210−215
37. Mecham RP, Gibson MA: The microfibril-associated glycoproteins (MAGPs) and the microfibrillar niche. Matrix Biol 2015, 47:13−33
38. Wiggs JL, Pawlyk B, Connolly E, Adamian M, Miller JW, Pasquale LR, Haddadin RI, Grosskreutz CL, Rhee DJ, Li T: Disruption of the blood−aqueous barrier and lens abnormalities in mice lacking lysyl oxidase-like 1 (LOXL1). Invest Ophthalmol Vis Sci 2014, 55:856−864
39. Li G, Schmitt H, Johnson WM, Lee C, Navarro I, Cui J, Fleming T, Gomez-Caraballo M, Elliott MH, Sherwood JM, Hauser MA, Farsiu S, Ethier CR, Stamer WD: Integral role for lysyl oxidase-like-1 in conventional outflow tissue function and behavior. FASEB J 2020, 34:10762−10777
40. Zadravec P, Braunger BM, Melzer B, Kroeber M, Bösl MR, Jägle H, Schlötzer-Schrehardt U, Tamm ER: Transgenic lysyl oxidase homolog 1 overexpression in the mouse eye results in the formation and release of protein aggregates. Exp Eye Res 2019, 179:115−124
41. Hewitt AW, Sharma S, Burdon KP, Wang JJ, Baird PN, Dimasi DP, Mackey DA, Mitchell P, Craig JE: Ancestral LOXL1 variants are associated with pseudoexfoliation in Caucasian Australians but with markedly lower penetrance than in Nordic people. Hum Mol Genet 2008, 17:710−716
42. Urban Z, Agapova O, Hucthagowder V, Yang P, Starcher BC, Hernandez MR: Population differences in elastin maturation in optic nerve head tissue and astrocytes. Invest Ophthalmol Vis Sci 2007, 48: 3209−3215
43. Ma H-Y, Li Q, Wong WR, N'Diaye E-N, Caplazi P, Bender H, Huang Z, Arlantico A, Jeet S, Wong A, Emson C, Brightbill H, Tam L, Newman R, Roose-Girma M, Sandoval W, Ding N: LOXL4, but not LOXL2, is the critical determinant of pathological collagen cross-linking and fibrosis in the lung. Sci Adv 2023, 9:eadf0133
44. Vranka JA, Kelley MJ, Acott TS, Keller KE: Extracellular matrix in the trabecular meshwork: intraocular pressure regulation and dysregulation in glaucoma. Exp Eye Res 2015, 133:112−125
45. Hann CR, Fautsch MP: The elastin fiber system between and adjacent to collector channels in the human juxtacanalicular tissue. Invest Ophthalmol Vis Sci 2011, 52:45−50
46. Navneet S, Rohrer B: Elastin turnover in ocular diseases: a special focus on age-related macular degeneration. Exp Eye Res 2022, 222: 109164
47. Morrison JC, Cepurna Ying Guo WO, Johnson EC: Pathophysiology of human glaucomatous optic nerve damage: insights from rodent models of glaucoma. Exp Eye Res 2011, 93:156−164
48. Quigley HA, Brown A, Dorman-Pease ME: Alterations in elastin of the optic nerve head in human and experimental glaucoma. Br J Ophthalmol 1991, 75:552−557